

Tumbling motion of magnetic particles on a magnetic substrate induced by a rotational magnetic field

Hisao Morimoto,¹ Tomofumi Ukai,¹ Yutaka Nagaoka,¹ Nicole Grobert,² and Toru Maekawa^{1,*}
¹*Bio-Nano Electronics Research Center, Toyo University, 2100 Kujirai, Kawagoe, Saitama 350-8585, Japan*
²*Department of Materials, University of Oxford, Parks Road, Oxford OX1 3PH, United Kingdom*
 (Received 14 February 2008; revised manuscript received 20 June 2008; published 8 August 2008)

We analyze the dynamics of paramagnetic particles on a paramagnetic substrate under a rotational magnetic field. When the paramagnetic particles are subjected to a rotational magnetic field, the rotational plane of which is perpendicular to the substrate surface, the particles form chain clusters caused by the dipole-dipole interaction between the particles and these clusters display a tumbling motion under certain conditions. In this case, the angular momentum of the clusters is converted to a translational one through the force of friction acting between the particles and substrate and, as a result, the clusters move along the surface of the substrate. We analyze the conditions under which the tumbling motion occurs and the dependence of the translational velocity of a cluster on the control parameters by the Stokesian dynamics method. Based on the dynamics of magnetic particles, we propose a method of manipulating nano- and microparticles using a rotational magnetic field. We demonstrate the manipulation of magnetic and nonmagnetic particles, a carbon nanotube, and a biological cell.

DOI: 10.1103/PhysRevE.78.021403

PACS number(s): 82.70.-y, 45.50.-j, 83.80.Gv, 87.80.Fe

It is well known that magnetic colloidal particles subjected to a dc magnetic field form chain clusters along the field direction. If the direction of the field is rotated, the clusters rotate, following the field rotation [1–6]. As the frequency of the rotational field increases, the rotating clusters are dissociated into shorter ones due to viscous drag. However, when the number density of particles is relatively high, the short rotating clusters coagulate together to form isotropic disklike clusters in the plane of the field rotation [2]. The disklike clusters rotate much more slowly than the field rotation. Nagaoka, Morimoto, and Maekawa observed that the particles near the surface of the disklike clusters form short rod clusters, which rotate following the field rotation, and these clusters circulate along the surface of the disklike clusters [2]. This experimental observation suggests that, if magnetic particles placed on a magnetic substrate are subjected to a rotational magnetic field, the rotational plane of which is perpendicular to the surface of the substrate, a similar motion to that observed on the surface of the disklike clusters may be induced along the substrate, which we call a “tumbling motion” (see Fig. 1). Although several researchers have investigated the dynamics of magnetic particles and magnetic holes (nonmagnetic particles dispersed in magnetic fluid) placed on magnetically patterned substrates under rotating magnetic fields recently [7–9], the tumbling motion of particles has not yet been reported. In this paper, we study the dynamics of magnetic particles on a magnetic substrate and clarify the conditions, under which the tumbling motion occurs. By utilizing the tumbling motion induced by the rotational magnetic field, magnetic particles can be moved along the surface of a magnetic substrate. The direction of the movement along the substrate can be altered by changing the direction of the rotational axis of the external magnetic field and therefore the particles can be positioned anywhere on the

substrate. Even nonmagnetic particles can be moved if they are dispersed in a paramagnetic solution such as a magnetic fluid, magnetic ionic liquid [10], or aqueous solution of paramagnetic ions [for instance, gadolinium (III) salt solution, which has a high magnetic susceptibility and is biologically benign [11]], in which case the particles behave as magnetic holes [12]. We propose a method of manipulating nanomicroscale objects utilizing the tumbling motion of particles induced by a rotational magnetic field and demonstrate the manipulation of magnetic and nonmagnetic particles, a carbon nanotube, and a biological cell.

The analytical system in this study is shown in Fig. 1. We

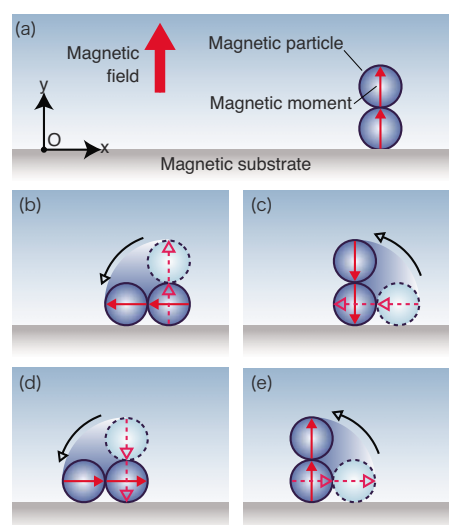


FIG. 1. (Color online) Tumbling motion of magnetic particles along a magnetic substrate induced by a rotational magnetic field. A cluster composed of magnetic particles on a magnetic substrate rotates following the rotation of the magnetic field. When the frictional force acting between the particle and the substrate is sufficiently large, the cluster moves along the substrate surface.

*Corresponding author. maekawa@toyonet.toyo.ac.jp

focus on the following case: (a) a cluster composed of two paramagnetic particles is placed on a paramagnetic substrate and (b) a magnetic substrate extends infinitely both horizontally and downward (see Fig. 1). Considering the existence of the magnetic substrate and the demagnetization effect in each particle, the magnetic dipole moment induced in magnetic particle i is expressed by the following equation [5,13]:

$$\mathbf{m}_i = \frac{6V\mu_f(\mu_p - \mu_f)}{(\mu_p + 2\mu_f)(\mu_s + \mu_f)} \begin{pmatrix} \mu_f & 0 \\ 0 & \mu_s \end{pmatrix} \mathbf{H}, \quad (1)$$

where \mathbf{H} , V , μ_p , μ_s , and μ_f are the external magnetic field, the volume of a magnetic particle, and the permeabilities of the magnetic particle, the magnetic substrate, and the solvent fluid, respectively. The force acting on particle i through the dipole-dipole interaction with the other particles, \mathbf{F}_i^{dp} , is expressed as follows [14–16]:

$$\mathbf{F}_i^{\text{dp}} = \sum_{j=1(j \neq i)}^N \frac{3|\mathbf{m}_i|^2}{4\pi\mu_f} \left(\frac{\mathbf{r}_{ij}}{r_{ij}^5} (1 - 5 \cos^2 \theta_{ij}) + \frac{2\mathbf{m}_i}{|\mathbf{m}_i|r_{ij}^4} \cos \theta_{ij} \right), \quad (2)$$

where \mathbf{r}_{ij} and θ_{ij} are, respectively, the vector directed from the position of particle j to that of particle i and the angle between the vectors \mathbf{m}_i and \mathbf{r}_{ij} . When magnetic particles are placed on a magnetic substrate, the images of the particles are produced in the substrate. The position and dipole moment vector of the image of particle i , which are denoted by \mathbf{r}_i^* and \mathbf{m}_i^* , are given in [13]:

$$\mathbf{r}_i^* = \begin{pmatrix} 1 & 0 \\ 0 & -1 \end{pmatrix} \mathbf{r}_i, \quad \mathbf{m}_i^* = \begin{pmatrix} -|k_s| & 0 \\ 0 & |k_s| \end{pmatrix} \mathbf{m}_i, \quad (3)$$

where \mathbf{r}_i is the position vector of particle i . k_s is defined as $k_s \equiv (\mu_s - \mu_f)/(\mu_s + \mu_f)$. The magnetic force acting on particle i through the interaction with the substrate, \mathbf{F}_i^{ds} , is expressed by the summation of the magnetic force through the interaction with the images of the particles produced in the substrate [13],

$$\mathbf{F}_i^{\text{ds}} = \sum_{j=1}^N \frac{1}{4\pi\mu_f} \left(\frac{3(\mathbf{m}_i \cdot \mathbf{m}_j^*)\mathbf{r}_{ij}^*}{r_{ij}^{*5}} - \frac{15\mathbf{r}_{ij}^*}{r_{ij}^{*7}} (\mathbf{m}_i \cdot \mathbf{r}_{ij}^*)(\mathbf{m}_j^* \cdot \mathbf{r}_{ij}^*) \right. \\ \left. + \frac{3\mathbf{m}_i}{r_{ij}^{*5}} (\mathbf{m}_j^* \cdot \mathbf{r}_{ij}^*) + \frac{3\mathbf{m}_j^*}{r_{ij}^{*5}} (\mathbf{m}_i \cdot \mathbf{r}_{ij}^*) \right). \quad (4)$$

Here, N is the number of particles in the system ($N=2$ in the present case). \mathbf{r}_{ij} and \mathbf{r}_{ij}^* are the vectors defined as $\mathbf{r}_{ij} = \mathbf{r}_i - \mathbf{r}_j$ and $\mathbf{r}_{ij}^* = \mathbf{r}_i - \mathbf{r}_j^*$. The magnetic particle-particle interaction force [Eq. (2)] is the internal force of the particles' system and therefore this force does not contribute to the movement of the center of mass of the system. The total force acting on the magnetic particles through the magnetic interaction with the substrate, on the other hand, can move the center of mass of the system. Now we divide the total force acting between a particle and the substrate into the interaction force acting between a particle and its image and that between a particle and the image of the other particles. The former is always perpendicular to the substrate surface [see Eq. (4)], whereas the latter possesses a horizontal component. However, the

horizontal component of the force acting on particle i through the interaction with the image of particle j is canceled out by that acting on particle j through the interaction with the image of particle i , which can be confirmed by Eq. (4), and, as a result, the total force acting on the magnetic particles through the interaction with the substrate is always perpendicular to the substrate surface. This means that the magnetic force acting on the magnetic particles does not directly contribute to the movement of the cluster in the horizontal direction. An external horizontal force can be applied to the system via the friction between the particles and substrate and the cluster can be moved in the horizontal direction through the tumbling motion as is shown in Fig. 1. As the permeability of the substrate increases, in which case k_s also increases, the cluster can be moved efficiently in the horizontal direction since the friction force acting between the particles and substrate is proportional to the normal force. However, when k_s is very high, the cluster cannot keep up the tumbling motion due to the strong attractive force from the substrate. For a smooth tumbling motion, the chain cluster must consistently repeat a series of standing-up and falling-down motions along the substrate [see Figs. 1(b)–1(e)]. Therefore, to realize the tumbling motion, the cluster has to be pulled up by the rotational magnetic field overcoming the attraction from the substrate. Now, we consider the chain cluster composed of two particles, both of which contact the substrate, and estimate the force acting on the particles. When the cluster stands up, one particle maintains contact with the substrate and the other one is lifted up [see Figs. 1(c) and 1(e)]. Therefore, the total force acting on the latter particle should be upward. The total force acting on the particle changes depending on the direction of the magnetic field and the maximal value of the y component of the force is positive when $k_s < 0.84$. Therefore, k_s should at least be less than 0.84 to realize the tumbling motion of the cluster. To analyze the efficient conditions for producing the tumbling motion in more detail, we carry out a Stokesian dynamics simulation of the particles' movement. In this analysis, we introduce additional repulsive forces acting on particle i induced by the other particles, \mathbf{F}_i^{rp} , and that induced by the substrate, \mathbf{F}_i^{rs} [17]:

$$\mathbf{F}_i^{\text{rp}} = \sum_{j=1(j \neq i)}^N \frac{6|\mathbf{m}_i|^2}{4\pi\mu_f d^4} \exp \left[-60 \left(\frac{r_{ij}}{d} - 1 \right) \right] \frac{\mathbf{r}_{ij}}{r_{ij}}, \quad (5)$$

$$\mathbf{F}_i^{\text{rs}} = \frac{3k_s |\mathbf{m}_i|^2 (2 - \cos^2 \varphi_i)}{4\pi\mu_f d^4} \exp \left[-60 \left(\frac{2y_i}{d} - 1 \right) \right] \mathbf{e}_y, \quad (6)$$

where d , φ_i , y_i , and \mathbf{e}_y are the diameter of a particle, the angle between a magnetic moment and the surface of the substrate, the distance between the center of particle i and the surface of the substrate, and the unit vector in the y direction. We assume that a frictional force acts between a particle and the substrate when the following conditions are satisfied. (i) $y_i \leq 0.55d$. (ii) The force acting on the particle has a downward component. The friction force acting between particle i and the substrate is given by $\mathbf{F}_i^{\text{fs}} = -(v_{ix}/|v_{ix}|)\eta_s|F_d|\mathbf{e}_x$, where v_{ix} , η_s , F_d , and \mathbf{e}_x are the x component of the velocity of particle i , the coefficient of dynamic friction, the downward

component of the force acting on particle i , and the unit vector in the x direction, respectively. Since the diameter of the particles we focus on ranges from nanometer to micrometer, the inertial effect in the particles' motions is negligible [18]. Therefore, the equation of motion can be expressed as $\mathbf{v}_i(t) = \mathbf{F}_i(t) / \zeta$, where t , \mathbf{F}_i , and ζ are the time, the total force acting on particle i ($= \mathbf{F}_i^{\text{dp}} + \mathbf{F}_i^{\text{ds}} + \mathbf{F}_i^{\text{rp}} + \mathbf{F}_i^{\text{rs}} + \mathbf{F}_i^{\text{fs}}$), and the Stokes friction coefficient, $\zeta = 3\pi\eta_f d$. η_f is the dynamic viscosity of the solvent. We nondimensionalize the coordinate, the time, and the force by d , $1/\omega$, and $3\pi\eta_f d^2 \omega$, respectively, where ω is the angular frequency of the rotational magnetic field. By nondimensionalizing the equation of motion, the following three nondimensional control parameters are derived: the Mason number $\text{Ma} \equiv 12^2 \mu_f \eta_f \omega / M^2$, which is the ratio of the viscous force to magnetic force, the nondimensional parameter k_s , which represents the strength of the dipole-dipole interaction between a particle and the substrate, and the coefficient of dynamic friction between a particle and the substrate, η_s . M is the magnetization of the particle in the absence of a magnetic substrate. We integrate the nondimensional equation of motion numerically for different combinations of the control parameters based on the procedures used by Mohebi, Jamasbi, and Liu [18].

According to Melle *et al.* [4], rotating chain clusters, which are subjected to a rotational magnetic field, are dissociated into single particles when Ma is greater than 1. As we mentioned above, to realize the tumbling motion of the cluster, k_s should be less than 0.84. Therefore, in this analysis, we focus on the following conditions: $\text{Ma} < 1$ and $k_s < 0.84$. When $\eta_s = 0$ (nonfriction), the cluster simply rotates around the center of inertia. The rotating cluster does not move in the horizontal direction but the cluster moves in the vertical direction when k_s is relatively high. In the case of $\eta_s \neq 0$, on the other hand, the cluster moves along the substrate surface via the tumbling motion. Generally speaking, as η_s increases, the cluster can move more efficiently. The typical movement of two paramagnetic particles along a paramagnetic substrate in the case of $\eta_s = 0.5$ obtained by the present simulations are shown in Figs. 2(a)–2(c) [19]. In the most efficient case, the translational displacement of the cluster during one cycle of a rotational magnetic field is $2d$, where d is the diameter of the particle [see Fig. 2(a)]. When the system is subjected to a high-frequency magnetic field (high Ma), or when the cluster is placed on a substrate of low magnetic permeability (low k_s), the translational displacement of the cluster becomes shorter than $2d$ [see Figs. 2(b) and 2(c)]. Figure 2(d) shows the nondimensional translational displacement L of the cluster during one cycle of the rotational magnetic field as a function of the nondimensional parameters Ma and k_s , where the translational displacement is normalized by that in the most efficient case, that is, $2d$. The normalized displacement of a cluster increases as the frequency (Ma) decreases and the permeability of the substrate (k_s) increases. The dependence of L on Ma and k_s in different η_s cases is qualitatively the same as that shown in Fig. 2(d). It is worth discussing the dynamics of ferromagnetic particles on a paramagnetic substrate. In the case of ferromagnetic particles, a single particle can be rotated by applying a rotational magnetic field since the particle possesses a permanent dipole moment or rema-

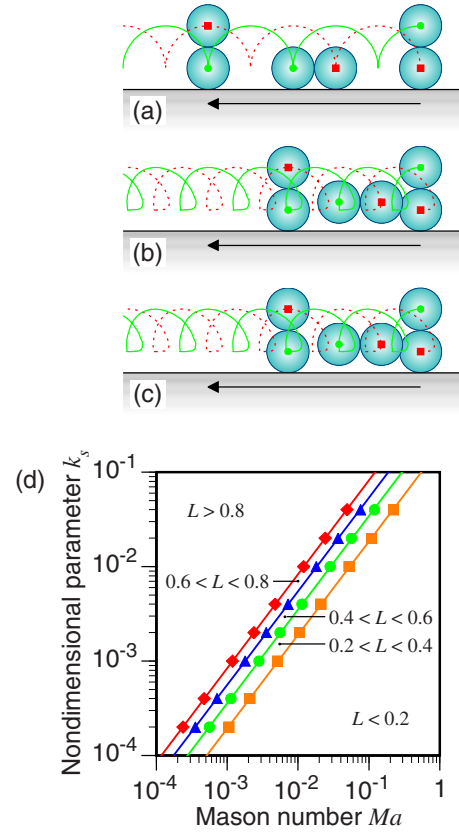


FIG. 2. (Color online) Dynamics of a cluster composed of two paramagnetic particles obtained by the Stokesian dynamics method. The coefficient of dynamic friction, η_s , is 0.5. (a)–(c) show the trajectories of each particle: (a) $k_s = 1.0 \times 10^{-2}$, $\text{Ma} = 1.0 \times 10^{-3}$; (b) $k_s = 1.0 \times 10^{-2}$, $\text{Ma} = 1.7 \times 10^{-2}$; (c) $k_s = 6.0 \times 10^{-4}$, $\text{Ma} = 1.0 \times 10^{-3}$. The magnetic field rotates in a counterclockwise direction and the clusters are moved from right to left. The snapshots in each figure from the right correspond to the 0th, 1.25th, and 2.5th cycles of the rotational magnetic field. (d) shows the isolines of the translational displacement L of the cluster during one cycle of the magnetic field, which is normalized by that in the most efficient case (2d), as a function of k_s and Ma . $L = \blacksquare$ 0.2; \bullet 0.4; \blacktriangle 0.6; \blacklozenge 0.8. The solid lines are guides for the eye.

nant magnetization and thus the torque acts on the particle through the interaction between the dipole moment of the particle and the external magnetic field. The interactive force between the particle and paramagnetic substrate is always attractive during the particle's rotation. Therefore, when the friction between the particle and substrate is sufficiently large, a single ferromagnetic particle can be moved along the surface of the substrate.

We carried out experiments of the movement of magnetic particles on a magnetic substrate under a rotational magnetic field [19]. Schematic representations of our manipulation test cell and experimental system are shown in Fig. 3. Paramagnetic particles (PMPs) (Dynabeads M-270 carboxylic acid; Dynal Biotech Ltd.) were dispersed in water. The diameter and magnetic susceptibility of each particle were, respectively, $2.8 \mu\text{m}$ and $2.2 \times 10^{-7} \text{ H/m}$. The test cell was composed of a magnetic film (cobalt-dispersed polyester film) and the aqueous solution of PMPs, which were sandwiched

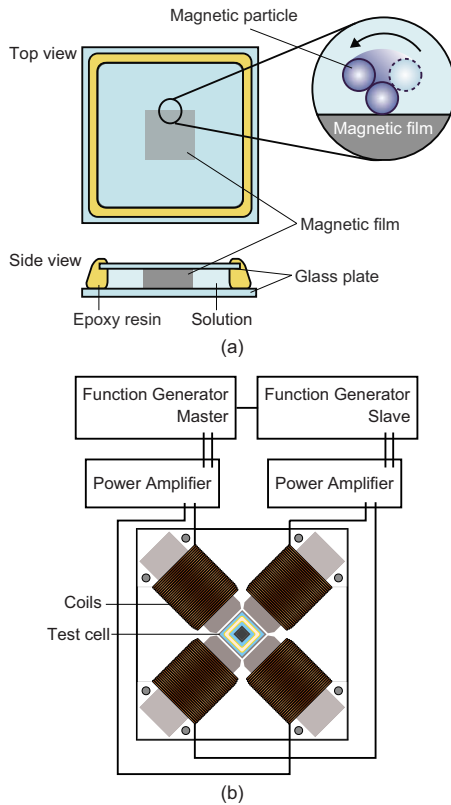


FIG. 3. (Color online) Experimental system. (a) Manipulation test cell. A magnetic film is sandwiched between two glass plates. Solution, in which magnetic particles are dispersed, is introduced into the test cell and particles are manipulated along the peripheral surface of the magnetic film. (b) Whole system. The test cell is placed on a horizontal plate surrounded by two pairs of coils. A rotational magnetic field is generated by the two pairs of coils, two function generators, and two amplifiers. The dynamics of the particles are recorded on both the hard disk of a computer and videotape.

between two glass plates [see Fig. 3(a)]. The thickness and magnetic susceptibility of the film were $7 \mu\text{m}$ and $2.2 \times 10^{-8} \text{ H/m}$. We used two pairs of coils, two function generators, and two amplifiers to generate a homogeneous rotational magnetic field [see Fig. 3(b)]. We placed the test cell on a horizontal plate surrounded by the two pairs of coils so that the rotational plane of the field was in parallel to the magnetic film [Fig. 3(b)] and observed the particles' tumbling motion along the peripheral surface of the film [Fig. 3(a)] using a charged-couple-device high-speed video camera, which was connected to both a computer and videotape recorder. The dynamics of the particles was recorded on both the hard disk of the computer and videotape. Figures 4(a) and 4(b) show the movement of chain clusters composed of two and five paramagnetic particles along the magnetic film. A magnetic field of 12.7 kA/m , which corresponds to a magnetic flux density of 16 mT , was rotated at a frequency of 1.0 Hz in a counterclockwise direction and the clusters were made to move from right to left, rotating in a counterclockwise direction. The above experimental conditions correspond to $\text{Ma}=0.14$ and $k_s=8.7 \times 10^{-3}$. As the theoretical result suggested, paramagnetic microparticles can be moved in

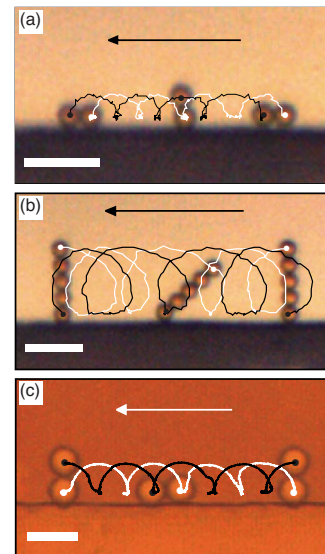


FIG. 4. (Color online) Tumbling motions of microparticles in rotational magnetic fields. The intensity of the magnetic field, which is rotated in a counterclockwise direction, is 12.7 kA/m . (a) Movement of a chain cluster composed of two paramagnetic particles. The diameter and magnetic susceptibility of each particle are $2.8 \mu\text{m}$ and $2.2 \times 10^{-7} \text{ H/m}$. The magnetic susceptibility of the substrate is $2.2 \times 10^{-8} \text{ H/m}$. The frequency of the field is 1 Hz . The trajectories of the two particles are drawn and the snapshots from the right correspond to the 0th, 1.8th, and 4.0th cycles of the rotational magnetic field. The scale bar represents $10 \mu\text{m}$. (b) Movement of a chain cluster composed of five paramagnetic particles. The frequency of the field is 1 Hz . The trajectories of the particles at the tip of the cluster are drawn and the snapshots from the right correspond to the 0th, 1.8th, and 4.0th cycles of the rotational magnetic field. The scale bar represents $10 \mu\text{m}$. (c) Movement of non-magnetic polystyrene particles along a nonmagnetic polystyrene substrate. The diameter of each particle is $6.0 \mu\text{m}$. The particles are dispersed in a magnetic fluid. The susceptibility of the fluid is $1.2 \times 10^{-7} \text{ H/m}$. The frequency of the field is 0.1 Hz . The trajectories of the two particles are drawn and the snapshots from the right correspond to the 0th, 2.3th, and 4.0th cycles of the rotational magnetic field. The scale bar represents $10 \mu\text{m}$.

low-frequency (low-Ma) and high-substrate-permeability (high- k_s) regions [see Fig. 2(d)]. It is difficult to compare the experimental result with the theoretical one from a quantitative point of view since the coefficient of dynamic friction between a particle and the substrate, η_s , is unknown in the experiment. According to the theoretical analysis, the translational displacement of a cluster composed of two magnetic particles during one cycle of the rotational field, L , increases with an increase in η_s ; e.g., L varies from 6.4×10^{-2} to 4.0×10^{-1} according to $0.5 \leq \eta_s \leq \infty$ in the case of $\text{Ma}=0.14$ and $k_s=8.7 \times 10^{-3}$, which corresponds to the present experimental conditions. Note that $\eta_s=\infty$ means that a particle does not move in the horizontal direction when the friction force acts between the particle and substrate. The average displacement obtained by the above experiment was 1.0 , which is greater than the theoretical value in the most efficient case, that is, $\eta_s=\infty$. This difference may be attributed to a finite-size effect of the magnetic substrate. As we mentioned in the above, in our experiment, we used a thin magnetic film and observed

the tumbling motion of the particles along the peripheral surface of the film for a clear visualization of the particles' dynamics. Therefore, the effect of the field gradient caused by the finite-size magnetic film on the tumbling motion may not be negligible. Note that in our analytical system the substrate extends infinitely in both the horizontal direction and downward. To realize a smooth tumbling motion of a cluster, the bottom particle of the cluster should not slide along the substrate during the standing-up and falling-down motions [see Figs. 2(b) and 2(c)]. Even in the case of $\eta_s = \infty$, the bottom particle slides if the magnetic attractive force acting on it from the substrate is weaker than the upward force caused by the upper particle, in which case the vertical component of the force acting on the bottom particle becomes upward and, as a result, no friction force acts between the particle and substrate. In other words, a magnetic force acting on the bottom particle from the substrate has to be strong enough to prevent sliding. In our experiment, the bottom particle must have been attracted more strongly due to the field gradient caused by the finite-size effect and therefore the cluster moved more efficiently than the theoretical and numerical predictions. We will be analyzing both theoretically and numerically the effect of the thickness and depth of the magnetic substrate on the dynamics of the magnetic particles in detail.

We also carried out an experiment of the movement of nonmagnetic polystyrene particles, which were dispersed in magnetic fluid [19]. We used a polystyrene film of 12 μm in thickness instead of a magnetic film. When the system is subjected to an external magnetic field, an apparent dipole is induced in each particle and the substrate in the opposite direction to the external magnetic field and therefore the nonmagnetic particles can also be moved by rotational magnetic fields. Magnetic fluid (W-40; Taiho Industry Co. Ltd.) was diluted so that the magnetic susceptibility of the fluid became 1.2×10^{-7} H/m. Polystyrene particles, the diameter of which was 6.0 μm (4206A; Duke Scientific Corporation), were dispersed in the magnetic fluid. Figure 4(c) shows the movement of two polystyrene particles along the polystyrene substrate, where a magnetic field of 12.7 kA/m was rotated at a frequency of 0.1 Hz. Based on the apparent dipole moment m induced in the opposite direction to the magnetic field, which can be calculated from Eq. (1), the Mason number Ma and the nondimensional parameter k_s are estimated as $\text{Ma} = 7.6 \times 10^{-2}$ and $k_s = -4.4 \times 10^{-2}$ in the above experiment. Note that, in a magnetic hole system, k_s is negative in general. The dynamics of the particles in a negative- k_s case is the same as that in a positive- k_s case since L is an even function of k_s . Therefore, nonmagnetic particles can be moved by a rotational magnetic field under low- Ma and low- k_s (high- $|k_s|$) conditions [see Fig. 2(d)]. According to our theoretical analysis, L under the above experimental conditions varies from 6.5×10^{-1} to 8.7×10^{-1} , according to $0.5 \leq \eta_s \leq \infty$. The average displacement obtained by the experiment was 9.8×10^{-1} , which is greater than the theoretical value even in the case of $\eta_s = \infty$. This difference is also attributed to the field gradient induced by the finite-size film.

We carried out an experiment of the movement of carbon nanotubes (CNTs), in which iron atoms are contained, Fe@CNTs, along a magnetic substrate [19]. Fe@CNTs were

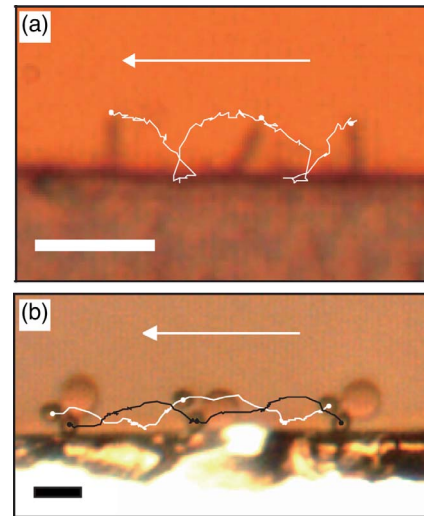


FIG. 5. (Color online) Manipulations of a carbon nanotube and a red blood cell. The intensity of the rotational magnetic field is 12.7 kA/m. (a) Movement of an iron-containing multiwalled carbon nanotube (Fe@CNT) along a magnetic substrate, the magnetic susceptibility of which is 2.6×10^{-5} H/m. The frequency of the field is 0.5 Hz. The trajectory of the tip of the Fe@CNT is drawn and the snapshots from the right correspond to the 0th, 1.1th, and 2.0th cycles of the rotational magnetic field. The scale bar represents 5 μm . (b) Movement of a sheep's red blood cell to which two magnetic particles are attached. The diameter and magnetic dipole moment of each particle in the field are 2.0 μm and 1.3×10^{-19} Wb m. The magnetic susceptibility of the film is 1.0×10^{-4} H/m. The frequency of the field is 0.5 Hz. The trajectories of the two magnetic particles are drawn and the snapshots from the right correspond to the 0th, 1.0th, and 2.1th cycles of the rotational magnetic field. The scale bar represents 5 μm .

produced by a chemical vapor deposition method, in which ferrocene was used as a catalyst. The details of the production of Fe@CNTs are explained elsewhere [20]. Fe@CNTs were dispersed in acetone and sonicated for 1 h. We used a nickel film as a magnetic substrate, the thickness and magnetic susceptibility of which were 10 μm and 2.6×10^{-5} H/m. Figure 5(a) shows the movement of a multiwalled Fe@CNT along the magnetic substrate, where a rotational magnetic field of 12.7 kA/m and 0.5 Hz was applied. The Fe@CNT was successfully moved from right to left, rotating in a counterclockwise direction in the rotational magnetic field.

Finally, we carried out the manipulation of a sheep's red blood cell (RBC) using a rotational magnetic field [19]. RBCs were separated from a sheep's whole blood by centrifugation and then dispersed in phosphate buffer saline (PBS; pH 7.4). Ferromagnetic particles (FMPs) of 2.0 μm in diameter (CFM-20-10; Spherotech Inc.) were dispersed in a different PBS after washing them with PBS several times, and the particle solution was filtered to remove aggregated particles. The particle solution was added to the RBC solution and, after shaking the mixed solution gently for 30 min at room temperature, the solution, in which FMP-RBC hybrids are dispersed, was introduced between the two glass plates for experiment. We used an iron film as a magnetic

substrate, the thickness and magnetic susceptibility of which were $10\ \mu\text{m}$ and $1.0 \times 10^{-4}\ \text{H/m}$. Figure 5(b) demonstrates the manipulation of a sheep's RBC, to which two FMPs were attached, in a rotational magnetic field of 0.5 Hz. The magnetic dipole moment of each particle in the magnetic field was $1.3 \times 10^{-19}\ \text{Wb m}$. The cell was manipulated successfully by the rotational magnetic field.

In summary, we used Stokesian dynamics simulation to analyze the tumbling motion of magnetic particles on a magnetic substrate in a rotational magnetic field theoretically and clarified the dependence of the rotational motion of clusters composed of magnetic particles on the Mason number Ma and nondimensional number k_s . We also carried out experiments of the movement of PMPs, nonmagnetic particles, an Fe@CNT, and a FMP-RBC hybrid, and found that they can be manipulated along magnetic substrates by utilizing the tumbling motion induced by a rotational magnetic field. Since the experimental conditions are not exactly the same as those of theoretical and numerical analyses, that is, the magnetic substrate extends infinitely both horizontally and downward in the theoretical and numerical analyses, whereas thin films were used in the experiments, a perfect quantitative agreement between the theoretical and experimental results was not obtained. In the case of a film of finite size, the local magnetic field is deformed and a magnetic field gradient is induced due to the finite-size effect, and therefore magnetic

particles are more firmly attracted to the substrate, which is favorable for the actual manipulations. However, it was confirmed by experiment that, when Ma is low and k_s is high, a smooth tumbling motion of magnetic particles is realized, which coincides well with the theoretical and numerical results. We will be investigating the tumbling motion of clusters along a magnetic substrate of finite size theoretically, numerically, and experimentally. We are convinced that biomolecules which are attached to magnetic particles and fullerenes in which magnetic atoms are contained can also be manipulated using the present method. Three-dimensional manipulation of nano- and micro-sized objects will be possible by using three pairs of magnets. The present manipulation method is so simple that it can easily be combined with other manipulation methods [21–34] and therefore will make a substantial contribution to progress in a wide range of science and technology.

This study has been supported by a Grant for the 21st Century Center of Excellence Program organized by the Ministry of Education, Culture, Sports, Science and Technology (MEXT), Japan, and the Inoue Enryo Memorial Foundation for Promoting Sciences, Toyo University. We would like to thank Akitoshi Eto for the fabrication of the magnetic films. T.U. and Y.N. would like to thank MEXT for financial support.

-
- [1] H. Singh, P. E. Laibinis, and T. A. Hatton, *Langmuir* **21**, 11500 (2005).
- [2] Y. Nagaoka, H. Morimoto, and T. Maekawa, *Phys. Rev. E* **71**, 032502 (2005).
- [3] S. L. Biswal and A. P. Gast, *Phys. Rev. E* **69**, 041406 (2004).
- [4] S. Melle, O. G. Calderón, M. A. Rubio, and G. G. Fuller, *Phys. Rev. E* **68**, 041503 (2003).
- [5] S. Melle, G. G. Fuller, and M. A. Rubio, *Phys. Rev. E* **61**, 4111 (2000).
- [6] O. Sandre, J. Browaeys, R. Perzynski, J.-C. Bacri, V. Cabuil, and R. E. Rosensweig, *Phys. Rev. E* **59**, 1736 (1999).
- [7] P. Tierno, T. H. Johansen, and T. M. Fischer, *Phys. Rev. Lett.* **99**, 038303 (2007).
- [8] D. Halverson, S. Kalghatgi, B. Yellen, and G. Friedman, *J. Appl. Phys.* **99**, 08P504 (2006).
- [9] B. B. Yellen, O. Hovorka, and G. Friedman, *Proc. Natl. Acad. Sci. U.S.A.* **102**, 8860 (2005).
- [10] M. Okuno, H. Hamaguchi, and S. Hayashi, *Appl. Phys. Lett.* **89**, 132506 (2006).
- [11] A. Winkleman, K. L. Gudiksen, D. Ryan, G. M. Whitesides, D. Greenfield, and M. Prentiss, *Appl. Phys. Lett.* **85**, 2411 (2004).
- [12] P. Pieranski, S. Clausen, G. Helgesen, and A. T. Skjeltorp, *Phys. Rev. Lett.* **77**, 1620 (1996).
- [13] L. D. Landau, E. M. Lifshitz, and L. P. Pitaevskii, *Electrodynamics of Continuous Media* (Pergamon, Oxford, 1984).
- [14] P. G. de Gennes and P. A. Pincus, *Phys. Kondens. Mater.* **11**, 189 (1970).
- [15] H. Morimoto and T. Maekawa, *J. Phys. A* **33**, 247 (2000).
- [16] H. Morimoto, T. Maekawa, and Y. Matsumoto, *Phys. Rev. E* **65**, 061508 (2002).
- [17] T. Ukai and T. Maekawa, *Phys. Rev. E* **69**, 032501 (2004).
- [18] M. Mohebi, N. Jamasbi, and J. Liu, *Phys. Rev. E* **54**, 5407 (1996).
- [19] See EPAPS Document No. E-PLLEE8-78-066808 for movies corresponding to Figs. 2(a)–2(c), 4(a)–4(c), 5(a), and 5(b). For more information on EPAPS, see <http://www.aip.org/pubservs/epaps.html>.
- [20] N. Grobert, W. K. Hsu, Y. Q. Zhu, J. P. Hare, H. W. Kroto, D. R. M. Walton, M. Terrones, H. Terrones, Ph. Redlich, M. Rühle, R. Escudero, and F. Morales, *Appl. Phys. Lett.* **75**, 3363 (1999).
- [21] D. G. Grier, *Nature (London)* **424**, 810 (2003).
- [22] A. LaPorta and M. D. Wang, *Phys. Rev. Lett.* **92**, 190801 (2004).
- [23] R. Krupke, F. Hennrich, H. v. Löhneysen, and M. M. Kappes, *Science* **301**, 344 (2003).
- [24] J. D. Beck, L. Shang, M. S. Marcus, and R. J. Hamers, *Nano Lett.* **5**, 777 (2005).
- [25] P. Y. Chiou, A. T. Ohta, and M. C. Wu, *Nature (London)* **436**, 370 (2005).
- [26] T. Deng, G. M. Whitesides, M. Radhakrishnan, G. Zabow, and M. Prentiss, *Appl. Phys. Lett.* **78**, 1775 (2001).
- [27] M. Tanase, D. M. Silevitch, A. Hultgren, L. A. Bauer, P. C. Searson, G. J. Meyer, and D. H. Reich, *J. Appl. Phys.* **91**, 8549 (2002).
- [28] L. E. Helseth, T. H. Johansen, and T. M. Fischer, *Phys. Rev. Lett.* **91**, 208302 (2003).
- [29] A. K. Bentley, J. S. Trethewey, A. B. Ellis, and W. C. Crone,

- Nano Lett. **4**, 487 (2004).
- [30] K. Han and A. B. Frazier, J. Appl. Phys. **96**, 5797 (2004).
- [31] H. Lee, A. M. Purdon, and R. M. Westervelt, Appl. Phys. Lett. **85**, 1063 (2004).
- [32] B. D. Matthews, D. A. LaVan, D. R. Overby, J. Karavitis, and D. E. Ingber, Appl. Phys. Lett. **85**, 2968 (2004).
- [33] P. Kim and C. M. Lieber, Science **286**, 2148 (1999).
- [34] Y. Mieda and K. Furutani, Phys. Rev. Lett. **95**, 177801 (2005).